Modernizing the open-source community Noah-MP land surface model (version 5.0) with enhanced modularity, interoperability, and applicability

Cenlin He[1], Prasanth Valayamkunnath[1,5], Michael Barlage[2], Fei Chen[1], David Gochis[1], Ryan Cabell[1], Tim Schneider[1], Roy Rasmussen[1], Guo-Yue Niu[3], Zong-Liang Yang[4], Dev Niyogi[4], Michael Ek[1]

[1]National Center for Atmospheric Research (NCAR), Boulder, Colorado, USA
[2]NOAA Environmental Modeling Center (EMC), College Park, Maryland, USA
[3]University of Arizona, Tucson, Arizona, USA
[4]University of Texas Austin, Austin, Texas, USA
[5]Indian Institute of Science Education and Research Thiruvananthapuram, India

Correspondence to: Cenlin He (cenlinhe@ucar.edu)

Abstract

The widely-used open-source community Noah-MP land surface model (LSM) is designed for applications ranging from uncoupled land-surface hydrometeorological and ecohydrological process studies to coupled numerical weather prediction and decadal global/regional climate simulations. It has been used in many coupled community weather/climate/hydrology models. In this study, we modernize/refactor the Noah-MP LSM by adopting modern Fortran code standards and data structures, which substantially enhances the model modularity, interoperability, and applicability. The modernized Noah-MP is released as the version 5.0 (v5.0), which has five key features: (1) enhanced modularization by re-organizing model physics into individual process-level Fortran module files, (2) enhanced data structure with new hierarchical data types and optimized variable declaration and initialization structures, (3) enhanced code structure and calling workflow by leveraging the new data structure and modularization, (4) enhanced (descriptive and self-explanatory) model variable naming standard, and (5) enhanced driver and interface structures to couple with host weather/climate/hydrology models. In addition, we create a comprehensive technical documentation of the Noah-MP v5.0 and a set of model benchmark and reference datasets. The Noah-MP v5.0 will be coupled to various weather/climate/hydrology models in the future. Overall, the modernized Noah-MP allows a more efficient and convenient process for future model developments and applications.

1. Introduction

Land surface models (LSMs) are useful modeling tools to resolve terrestrial responses to and interactions with the atmosphere, ocean, glacier, and sea ice in the earth system. Traditionally, LSMs were thought to mainly provide lower boundary conditions to the coupled atmospheric models. However, modern LSMs have been increasingly employed as indispensable components in the climate and weather systems to offer biogeophysical and biogeochemical insights for understanding and quantifying the impact and evolution of climate, weather, and the integrated earth environment (Blyth et al., 2021). LSMs have been widely applied to tackle many important societally relevant challenges, such as drought, flood, heat wave, water availability, agriculture, food security, wildfires, deforestation, and urbanization (Bonan and Doney, 2018).

Among many LSMs that have been developed in the past few decades, the open-source community Noah with Multi-parameterization Options (Noah-MP; Niu et al., 2011; Yang et al., 2011) is one of the most widely-used state-of-the-art LSMs. The article describing the Noah-MP model by Niu et al (2011) is *de facto* the most cited LSM paper in the last 10 years, highlighting its worldwide popular usage in the international science community. Compared to its predecessor, the Noah LSM (Chen et al., 1996, 1997; Chen and Dudhia, 2001; Ek et al., 2003), Noah-MP significantly improves known Noah limitations by employing enhanced treatments of vegetation canopy, snowpack, soil processes, groundwater, and their complex interactions as well as additional capabilities for critical land processes (e.g., crop, irrigation, tile drainage, groundwater, urban, carbon and nitrogen cycles). Another unique feature of Noah-MP is the inclusion of multiple physics options for different land processes, which allows the multi-physics model ensemble experiments for uncertainty assessment and testing competing hypotheses (Zhang et al., 2016; J. Li et al., 2020).

Noah-MP can be applied to various spatial scales spanning from point scale locally to ~100-km resolution globally, and temporal scales spanning from sub-daily to decadal time scales. Since its original development, Noah-MP has been used in many important applications, including numerical weather prediction (Suzuki and Zupanski, 2018; Ju et al., 2022), high-resolution climate modeling (Gao et al., 2017; Liu et al., 2017; Rasmussen et al., 2023), land data assimilation (Kumar et al., 2019; Xu et al., 2021; Nie et al., 2022; Shu et al., 2022), drought (Arsenault et al., 2020; Niu et al., 2020; Wu et al., 2021; Abolafia-Rosenzweig et al., 2023a), wildfire (Kumar et al., 2021; Abolafia-Rosenzweig et al., 2022a, 2023b), snowpack evolution (Wrzesien et al., 2015; He et al., 2019; Jiang et al., 2020), hydrology and water resources (Cai et al., 2014; Liang et al., 2019; X. Zhang et al., 2022a; Hazra et al., 2023), crop and agricultural management (Liu et al., 2016; Ingwersen et al., 2018; Warrach-Sagi et al., 2022; Valayamkunnath et al., 2022; Zhang et al., 2020, 2023), urbanization and heat island (Xu et al., 2018; Salamanca et al., 2018; Patel et al., 2022), biogeochemical cycle (Cai et al., 2016; Brunsell et al., 2021), wind erosion (Jiang et al., 2021),

wetland (Z. Zhang et al., 2022), groundwater (Barlage et al., 2015, 2021; Li et al., 2022), and landslide hazard (Zhuo et al., 2019).

Currently, Noah-MP has been implemented into many community research and operational weather/climate/hydrology models, including the Weather Research and Forecasting model (WRF), the Model for Prediction Across Scales (MPAS), the NOAA operational National Water Model (NWM), the NOAA Unified Forecast System (UFS), the NASA Land Information System (LIS), and the NCAR High-Resolution Land Data Assimilation System (HRLDAS).

Despite its popular usage in the international research and application communities, the Noah-MP core code engine was designed 12 years ago and is outdated, and does not take advantage of modern Fortran language architecture. It has a single lengthy (>12,000 lines) Fortran source file lumping together all model physics with complex code and data structures using inconsistent format and does not follow the modern Fortran 2003 code standard (https://j3-fortran.org/doc/year/04/04-007.pdf). This makes the Noah-MP model code difficult for users and developers to read, modify, and test as well as to implement and apply it to other community models. Furthermore, a lengthy code is error prone and challenging to debug. These issues limit the further development and application of Noah-MP.

Therefore, this effort is motivated to modernize (refactor) the entire Noah-MP model by adopting modern Fortran 2003 code standards and data structures, which substantially enhances the model modularity, interoperability, and applicability. The base code used for refactoring is the Noah-MP version 4.5 (released in December 2022; https://github.com/NCAR/noahmp/tree/release-v4.5-WRF), and the refactoring effort does not change model physics. We release the modernized/refactored Noah-MP as version 5.0 (v5.0; https://github.com/NCAR/noahmp), which includes five key features: (1) enhanced modularization by re-organizing model physics into individual process-level Fortran module files, (2) enhanced data structure with new hierarchical data types and optimized variable declaration and initialization structures, (3) enhanced code structure and subroutine calling workflow by leveraging the new data structure and modularization and refining code to be more concise, (4) enhanced (descriptive and self-explanatory) model variable naming standard, and (5) enhanced driver and interface code structures to couple with host weather/climate/hydrology models. In addition, we have created a comprehensive technical documentation (He et al., 2023) to describe model physics and details of the refactored Noah-MP and a set of model benchmark and reference datasets for future comparison and assessment. Overall, the modernized open-source community Noah-MP model (version 5.0) will allow a more efficient and convenient process for future model developments and applications. The framework and practice in the course of refactoring the entire Noah-MP code is also applicable to other LSMs and ESMs.

This paper reports the key features of the modernized Noah-MP v5.0 and is organized as follows. Section 2 briefly summarizes the Noah-MP model physics with several updates since its original development. Sections 3–7, respectively, introduce the key features of the modernized Noah-MP in terms of enhanced model modularization, data type, code structure, variable naming, and coupling structure with host models. Section 8 describes the model benchmarking and reference datasets. Section 9 provides the release information of model code and technical documentation. Section 10 concludes the paper with future model development plans.

2. Noah-MP version 5.0 model physics

2.1 Noah-MP description

Noah-MP (Niu et al., 2011) was originally developed based on the Noah LSM (Chen et al., 1996, 1997; Chen and Dudhia, 2001; Ek et al., 2003) to augment its modeling capabilities with enhanced physical representations and treatments of dynamic vegetation, canopy interception and radiative transfer processes, multi-layer snowpack physics, and soil and hydrological processes. The history of model development and evolution has been described in the technical documentation (He et al., 2023). Noah-MP is designed to simulate land surface and subsurface energy and water processes in both uncoupled and coupled modes with atmospheric or hydrological models at sub-daily time scale and high spatial resolution (even for point scale). This further allows the use of Noah-MP in different hydrological, weather, and climate models for applications in a wide range of spatial and temporal scales with proper integration in time and space.

The Noah-MP land grid is divided into two sub-grid tiles, namely vegetated and non-vegetated grounds, based on vegetation cover fraction. The biogeophysical and biogeochemical processes are treated separately for the vegetated and bare grounds. A "big-leaf" canopy treatment is adopted, which is characterized by canopy properties dependent on vegetation types. Noah-MP accounts for a multiple-layer snowpack, where snow ice and liquid water content, density, depth, and temperature are simulated dynamically. There are also multi-layer soil thermal and hydrological processes with dynamically evolving soil temperature and water content. The vegetation, snow, and soil components in Noah-MP are closely coupled and interacted with each other via complex energy, water, and biochemical processes. Their detailed physical formulations and parameterizations in Noah-MP v5.0 are described in the technical documentation (He et al., 2023). Below, we briefly summarize the energy, water, and biochemical processes in Noah-MP v5.0.

2.2 Noah-MP energy processes

Noah-MP resolves energy budgets and processes separately for vegetated and non-vegetated ground portions of each grid (Niu et al., 2011). The vegetation cover fraction, either from observational inputs or model calculations based on leaf area index (LAI) inputs or predicted by

the dynamic vegetation module, is used to separate vegetated and bare grounds. The grid-mean energy states and fluxes are calculated as an average of vegetated and bare ground values weighted by vegetation cover fraction. For surface radiative processes driven by incoming shortwave and longwave radiation (atmospheric forcing), Noah-MP simulates the radiative absorption and scattering by the canopy and ground (soil/snow) as well as the longwave emissions by the canopy and ground (soil/snow). The net absorbed total (shortwave and longwave) radiative flux is balanced by precipitation advected heat flux, total surface sensible and latent heat fluxes, and ground heat flux. The precipitation advected heat flux represents the heat flux advected from precipitation (rain/snow) to canopy/ground due to the temperature difference between precipitation (surface air) and canopy/ground. The total surface sensible heat includes the sensible heat from canopy, snowpack, and soil surfaces. The total surface latent heat includes the latent heat from snowpack sublimation, soil evaporation, canopy snow sublimation, canopy water evaporation, and plant transpiration. The ground heat flux is the heat flux leaving the ground surface to drive subsurface snow/soil phase change and/or temperature changes.

To model the aforementioned surface energy flux components, Noah-MP dynamically calculates a number of key land surface properties, include ground snow cover fraction, surface roughness, canopy and ground thermal properties, snow and soil albedo, surface emissivity, and canopy radiative transfer. Many of these property and process calculations have multiple physics options (see Sect. 2.6). Based on the canopy and ground energy balance, Noah-MP further solves the temperature and phase change for canopy, snowpack, and soil. Figure 1 summarizes the key energy processes and budget components as well as the energy balance equation in Noah-MP v5.0. Note that the energy processes at glacier grids are treated similarly to those at 100% bare (non-vegetated) ground grids except that the soil is replaced by glacier ice with ice-specific properties.

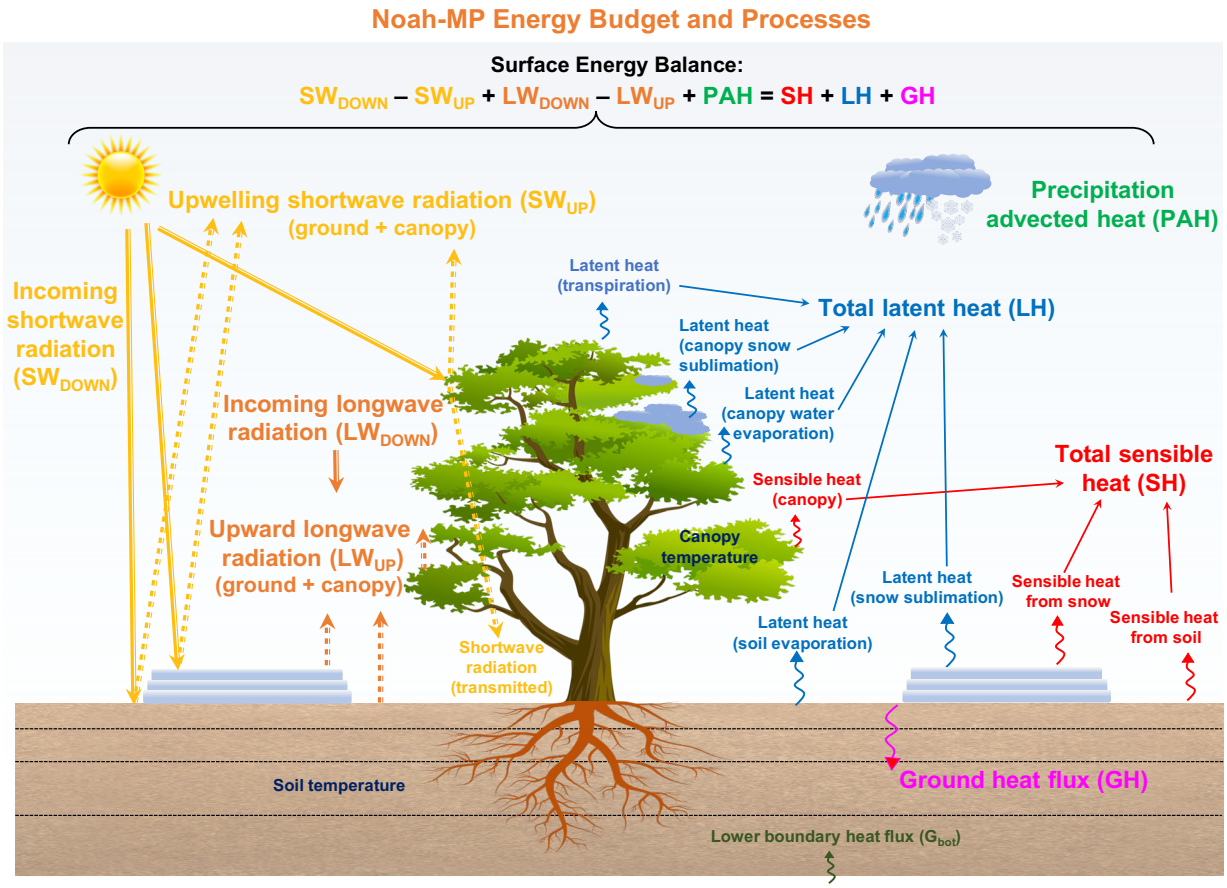

Figure 1. Schematic diagram of energy budget and processes represented in Noah-MP version 5.0.

2.3 Noah-MP water processes

Noah-MP accounts for five major water budget components, including precipitation, evapotranspiration (ET), total runoff, net lateral flow, and total water storage change intercepted by the canopy and in snow, soil, and aquifer. For precipitation, Noah-MP has several temperature-based rainfall-snowfall partitioning parameterizations or can use the partitioning from atmospheric models directly (see Sect. 2.6). Noah-MP simulates canopy interception and throughfall of rain and snow, where the intercepted rain and snow on the canopy can go through unloading/dripping, frost, sublimation, melting, and freezing processes. Net evaporation loss from the canopy-intercepted liquid water (evaporation minus dew), net sublimation from the canopy-intercepted snow (sublimation minus frost), transpiration (via plant hydraulics), net soil surface evaporation, and net snowpack sublimation together contribute to the total surface ET. Noah-MP dynamically simulates multi-layer snowpack water storage (ice and liquid water) changes driven by snowfall/rainfall, frost, sublimation, freezing, and melting. The snowmelt water out of snowpack together with rainfall at the soil surface are further partitioned into surface runoff and infiltration based on multiple runoff and infiltration physics options (see Sect. 2.6). Soil moisture and

unsaturated water flow across soil layers are simulated using the one-dimensional Richards equation. Two optional groundwater schemes, one without 2-D lateral flow (Niu et al., 2007) and one with 2-D lateral flow (Fan et al., 2007; Miguez-Macho et al. 2007), are available in Noah-MP to simulate groundwater dynamics, including groundwater recharge, water table change, baseflow, seepage, and/or lateral flow. Noah-MP also includes dynamic irrigation and tile drainage processes for agricultural management applications (Valayamkunnath et al., 2021, 2022). Figure 2 summarizes the key water processes and budget components as well as the water balance equation in Noah-MP v5.0. Note that the water processes at glacier grids are treated similarly to those at 100% bare ground grids except that all the soil and subsurface hydrological processes are removed and replaced by glacier ice (He et al., 2023).

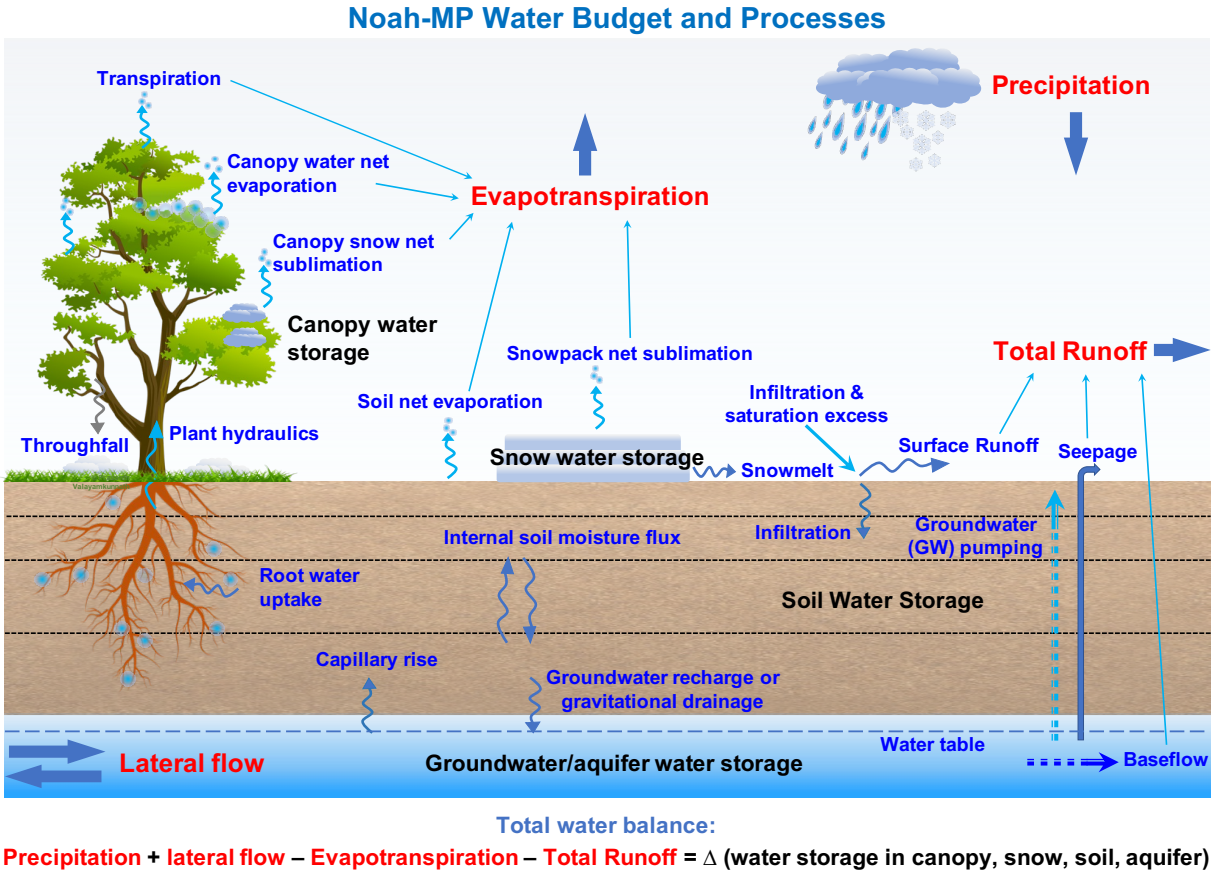

Figure 2. Schematic diagram of water budget and processes represented in Noah-MP version 5.0.

2.4 Noah-MP biochemical processes

Currently, the community version of Noah-MP only accounts for carbon processes for biochemical cycles, while nitrogen dynamics and soil carbon dynamics have been developed in non-community Noah-MP versions managed by individual research groups (e.g., Cai et al., 2016; X. Zhang et al.,

2022b). We will synthesize and integrate individual Noah-MP updates into the community version in the future (see Sect. 2.5 for more discussions). Noah-MP simulates carbon processes for both natural/generic vegetation (Niu et al., 2011) and explicit agricultural crops (Liu et al., 2016). The carbon processes related to vegetation growth dynamics include (1) carbon assimilation from photosynthesis by shaded and sunlit leaves, (2) carbon allocation to different parts of vegetation (leaf, stem, wood and root) and soil carbon pools (fast and slow carbon), (3) carbon loss due to respiration of different vegetation and soil carbon pools, (4) carbon transfer between vegetation and fast soil carbon pools through vegetation (leaf, stem, wood and root) turnover and seasonal death of leaf and stem, and (5) soil carbon pool conversion through soil carbon stabilization. The total carbon flux to the atmosphere and net primary productivity are computed based on the aforementioned carbon processes. Figure 3 summarizes the key carbon processes and budget components as well as the carbon balance equation in Noah-MP v5.0. Note that the carbon processes for crop growth are treated similarly to those of natural vegetation, except that the wood component of plants is removed and the grain component of crops is added with additional carbon conversion from leaf, stem, and root to grain depending on crop growing stages.

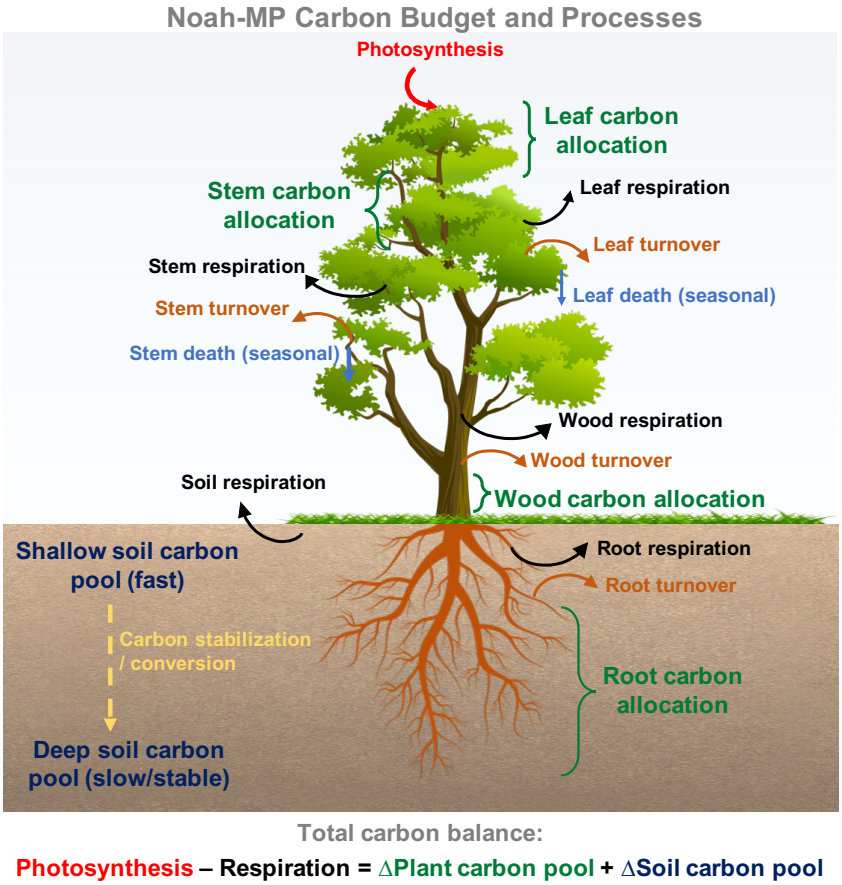

Figure 3. Schematic diagram of carbon budget and processes represented in Noah-MP version 5.0.

2.5 Noah-MP physics updates since original development

Since the release of the original Noah-MP in year 2011 (Niu et al., 2011), there are several important updates in Noah-MP physics. Some of the updates have been included in the community version of Noah-MP v5.0, while some are only available in the non-community versions managed by individual research groups. We will make efforts to synthesize and integrate individual Noah-MP updates into the community version in the future by working with those developer teams. Here, to the best of our knowledge, we briefly list the major Noah-MP physics updates from the community in the past decade.

The new/enhanced physics included in the community Noah-MP version 5.0 since 2011 are: (1) the Miguez-Macho-Fan (MMF) groundwater scheme (Barlage et al., 2015); (2) three additional runoff schemes: the Variable infiltration capacity (VIC), dynamic VIC, and Xinanjiang schemes (McDaniel et al., 2020); (3) tile drainage schemes (Valayamkunnath et al., 2022); (4) dynamic irrigation schemes (sprinkler, micro, and flooding irrigation) (Valayamkunnath et al., 2021); (5) a dynamic crop growth model for corn and soybean (Liu et al., 2016) with enhanced C3 and C4 crop parameters (Zhang et al., 2020); (6) coupling with urban canopy models (Xu et al., 2018; Salamanca et al., 2018) with local climate zone modeling capabilities (Zonato et al., 2021); (7) enhanced snow cover, snow compaction, and wind-canopy absorption parameters (He et al., 2021); (8) a wet-bulb temperature-based snow-rain partitioning scheme (Wang et al., 2019).

The new/enhanced physics currently not included in the community Noah-MP version 5.0 since 2011 are: (1) nitrogen dynamics (Cai et al., 2016); (2) big-tree plant hydraulics (Li et al., 2021); (3) dynamic root optimization (Wang et al. 2018) with an explicit representation of plant water storage (Niu et al., 2020); (4) additional snow cover parameterizations (Jiang et al., 2020); (5) coupling with a wind erosion model (Jiang et al., 2021); (6) a wetland representation and dynamics (Z. Zhang et al., 2022); (7) a unified turbulence parameterization throughout the canopy and roughness sublayer (Abolafia-Rosenzweig et al., 2021); (8) enhanced snow albedo representations (Abolafia-Rosenzweig et al., 2022b); (9) coupling with a snow radiative transfer (SNICAR) model (Wang et al., 2020, 2022); (10) an organic soil layer representation at forest floors (Chen et al., 2016) and a microbial-explicit soil organic carbon decomposition model (MESDM; X. Zhang et al., 2022b); (11) coupling with atmospheric dry deposition of air pollutant (Chang et al., 2022); (12) enhanced permafrost soil representations (X. Li et al., 2020); (13) spring wheat crop dynamics (Zhang et al., 2023); (14) new treatment of thermal roughness length (Chen and Zhang 2009); (15) the Gecros crop model (Ingwersen et al., 2018; Warrach-Sagi et al., 2022); (16) a 1-D dual-permeability flow model (based on the mixed-form Richards' equation) representing preferential flow through variably-saturated soil with surface ponding being developed at the University of Arizona.

2.6 Noah-MP multi-physics options

One unique feature and advantage of Noah-MP is the inclusion of multiple physics options for different land processes for testing competing hypotheses (i.e., options) and multi-model ensemble simulations. Table 1 summarizes all the available physics options in the community Noah-MP v5.0. In particular, compared to previous Noah-MP versions, we have separated the runoff options for surface and subsurface runoff processes, and added a new physics option for snow thermal conductivity calculations, which were originally hard-coded without the namelist control capability. More detailed descriptions of each physics option are provided in the technical documentation (He et al., 2023).

Table 1. List of Noah-MP version 5.0 multi-physics options

Noah-MP Physics	Option	Notes (* indicates the default option)
OptDynamicVeg options for dynamic (prognostic) vegetation	1	off (use table LeafAreaIndex; use VegFrac = VegFracGreen from input) (Niu et al., 2011; Yang et al., 2011)
	2	on (together with OptStomataResistance = 1) (Dickinson et al., 1998; Niu and Yang, 2003)
	3	off (use table LeafAreaIndex; calculate VegFrac)
	4*	off (use table LeafAreaIndex; use maximum vegetation fraction)
	5	on (use maximum vegetation fraction)
	6	on (use VegFrac = VegFracGreen from input)
	7	off (use input LeafAreaIndex; use VegFrac = VegFracGreen from input)
	8	off (use input LeafAreaIndex; calculate VegFrac)
	9	off (use input LeafAreaIndex; use maximum vegetation fraction)
OptRainSnowPartition options for partitioning precipitation into rainfall & snowfall	1*	Jordan (1991) scheme
	2	BATS: when TemperatureAirRefHeight < freezing point+2.2 (Yang and Dickinson, 1996)
	3	TemperatureAirRefHeight < freezing point (Niu et al., 2011)
	4	Use WRF microphysics output (Barlage et al., 2015)
	5	Use wet-bulb temperature (Wang et al., 2019)
OptSoilWaterTranspiration options for soil moisture factor for stomatal resistance & ET	1*	Noah (soil moisture) (Ek et al., 2003)
	2	CLM (matric potential) (Oleson et al., 2004)
	3	SSiB (matric potential) (Xue et al., 1991)
OptGroundResistanceEvap options for ground resistent to evaporation/sublimation	1*	Sakaguchi and Zeng (2009) scheme
	2	Sellers (1992) scheme
	3	adjusted Sellers (1992) for wet soil
	4	Sakaguchi and Zeng (2009) for non-snow; rsurf = rsurf_snow for snow (set in NoahmpTable.TBL)
OptSurfaceDrag options for surface layer drag/exchange coefficient	1*	Monin-Obukhov (M-O) Similarity Theory (Brutsaert, 1982)
	2	original Noah (Chen et al. 1997)

OptStomataResistance options for canopy stomatal resistance	1*	Ball-Berry scheme (Ball et al., 1987; Bonan, 1996)
	2	Jarvis scheme (Jarvis, 1976)
OptSnowAlbedo options for ground snow surface albedo	1*	BATS snow albedo (Dickinson et al., 1993)
	2	CLASS snow albedo (Verseghy, 1991)
OptCanopyRadiationTransfer options for canopy radiation transfer	1	modified two-stream (gap = *f* (solar angle,3D structure, etc) < 1-VegFrac) (Niu and Yang, 2004)
	2	two-stream applied to grid-cell (gap=0) (Niu et al., 2011)
	3*	two-stream applied to vegetated fraction (gap=1-VegFrac) (Dickinson, 1983; Sellers, 1985)
OptSnowSoilTempTime options for snow/soil temperature time scheme (only layer 1)	1*	semi-implicit; flux top boundary condition (Niu et al., 2011)
	2	full implicit (original Noah); temperature top boundary condition (Ek et al., 2003)
	3	same as 1, but snow cover for skin temperature calculation (Niu et al., 2011)
OptSnowThermConduct options for snow thermal conductivity	1*	Stieglitz scheme (Yen,1965)
	2	Anderson (1976) scheme
	3	Constant (Niu et al., 2011)
	4	Verseghy (1991) scheme
	5	Douvill scheme (Yen, 1981)
OptSoilTemperatureBottom options for lower boundary condition of soil temperature	1	zero heat flux from bottom (DepthSoilTempBottom & TemperatureSoilBottom not used) (Niu et al., 2011)
	2*	TemperatureSoilBottom at DepthSoilTempBottom (8m) read from a file (original Noah) (Ek et al., 2003)
OptSoilSupercoolWater options for soil supercooled liquid water	1*	No iteration (Niu and Yang, 2006)
	2	Koren's iteration (Koren et al., 1999)
OptRunoffSurface options for surface runoff	1	TOPMODEL with groundwater (Niu et al., 2007)
	2	TOPMODEL with an equilibrium water table (Niu et al., 2005)
	3*	Schaake scheme (original Noah) (Schaake et al., 1996)
	4	BATS surface and subsurface runoff (Yang and Dickinson, 1996)
	5	Miguez-Macho & Fan (MMF) groundwater scheme (Fan et al., 2007; Miguez-Macho et al. 2007)
	6	Variable Infiltration Capacity Model surface runoff scheme (Liang et al., 1994)
	7	Xinanjiang Infiltration and surface runoff scheme (Jayawardena and Zhou, 2000)
	8	Dynamic VIC surface runoff scheme (Liang and Xie, 2003)

OptRunoffSubsurface options for drainage & subsurface runoff	1~8	similar to runoff option, separated from original Noah-MP runoff option, currently tested & recommended the same option# as surface runoff (default)
OptSoilPermeabilityFrozen options for frozen soil permeability	1*	linear effects, more permeable (Niu and Yang, 2006)
	2	nonlinear effects, less permeable (Koren et al., 1999)
OptDynVicInfiltration options for infiltration in dynamic VIC runoff scheme	1*	Philip scheme (Liang and Xie, 2003)
	2	Green-Ampt scheme (Liang and Xie, 2003)
	3	Smith-Parlange scheme (Liang and Xie, 2003)
OptTileDrainage options for tile drainage currently only tested & calibrated to work with runoff option=3	0*	No tile drainage
	1	on (simple scheme) (Valayamkunnath et al., 2022)
	2	on (Hooghoudt's scheme) (Valayamkunnath et al., 2022)
OptIrrigation options for irrigation	0*	No irrigation
	1	Irrigation on (Valayamkunnath et al., 2021)
	2	irrigation trigger based on crop season planting and harvesting dates (Valayamkunnath et al., 2021)
	3	irrigation trigger based on LeafAreaIndex threshold (Valayamkunnath et al., 2021)
OptIrrigationMethod options for irrigation method, only works when OptIrrigation > 0	0*	method based on geo_em fractions
	1	sprinkler method (Valayamkunnath et al., 2021)
	2	micro/drip irrigation (Valayamkunnath et al., 2021)
	3	surface flooding (Valayamkunnath et al., 2021)
OptCropModel options for crop model	0*	No crop model
	1	Liu, et al. (2016) crop scheme
OptSoilProperty options for defining soil properties	1*	use input dominant soil texture
	2	use input soil texture that varies with depth
	3	use soil composition (sand, clay, orgm) and pedotransfer function
	4	use input soil properties
OptPedotransfer options for pedotransfer functions, only works when OptSoilProperty=3	1*	Saxton and Rawls (2006) scheme
OptGlacierTreatment options for glacier treatment	1*	include phase change of glacier ice
	2	Glacier ice treatment more like original Noah

3. Enhanced model modularization in Noah-MP version 5.0

In the Noah-MP v5.0, we have modularized all model physics by separating and re-organizing each code subroutine into individual process-level Fortran module file with new descriptive, self-

explanatory module and subroutine names. As such, each model physics or scheme has its own separate module. Figure 4 shows the calling tree of the modularized Noah-MP main model physics workflow. Figures 5-7 show the calling tree of the modularized energy, water, and carbon processes, respectively. Compared to the previous Noah-MP versions that have a single lengthy source file lumping together all model subroutines with non-self-explanatory names, the highly-modularized model structure of the Noah-MP v5.0 provides a much more clear, neat, and organized way for users and developers to understand and follow the model logics and physics. These new modules use consistent coding format and standards, offering convenience for code reading, writing, and debugging. The highly-modularized model structure facilitates future development by allowing specific model physics to be worked in isolation or replaced without interfering with other parts of the model code. This modularization also allows external community weather/climate/hydrology models to easily adopt specific Noah-MP physical processes/schemes as independent process-level module files and implement them for testing and coupling.

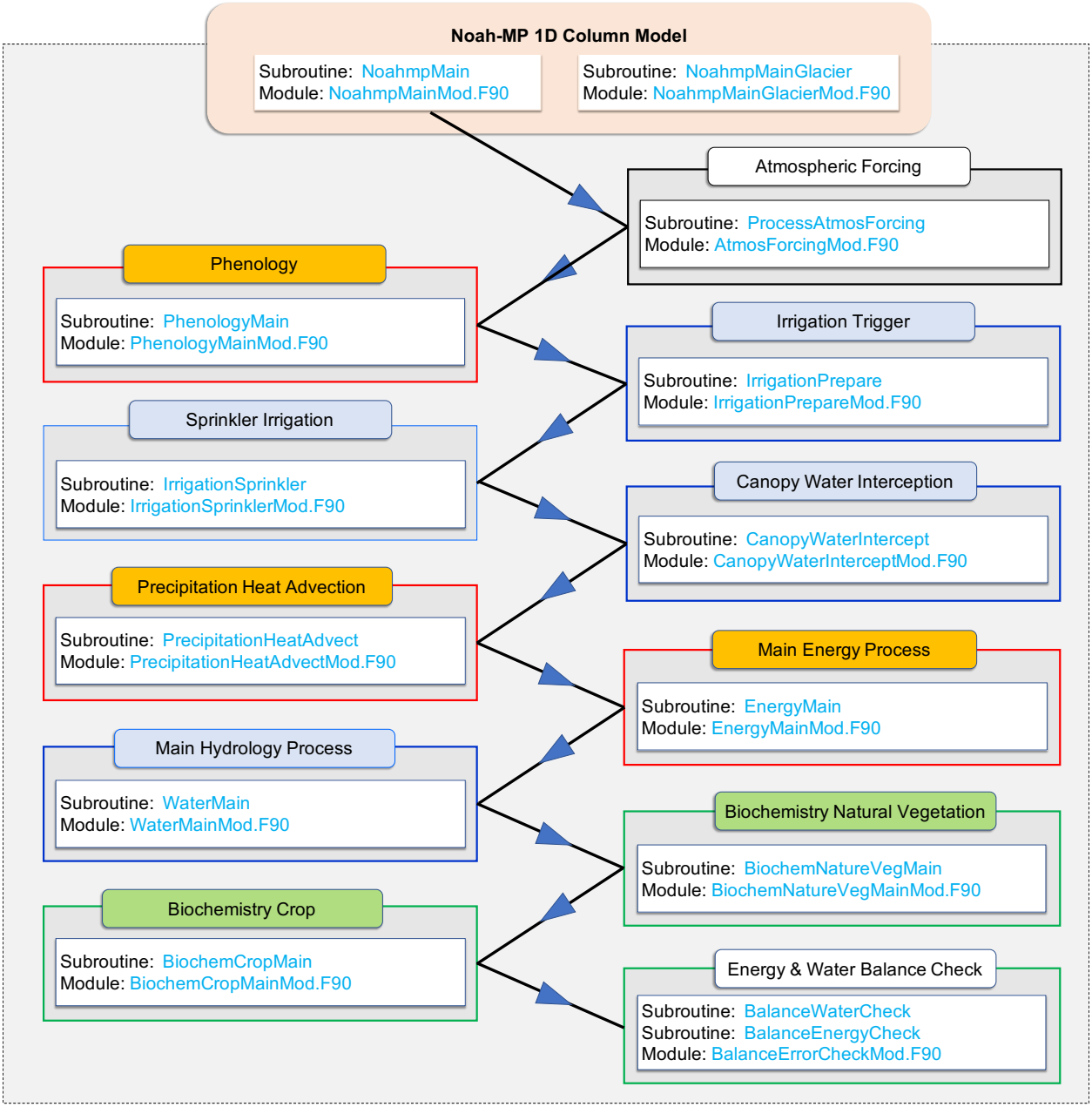

Figure 4. The modularized Noah-MP main physics calling tree in version 5.0. Blue boxes indicate water processes, orange boxes indicate energy processes, and green boxes indicate biochemical processes. The direction of arrows indicates processes calling sequence and information flow. Note that the 1-D glacier column model has similar structures as the main non-glacier model, except that the vegetation-related processes are removed and soil is replaced by glacier ice.

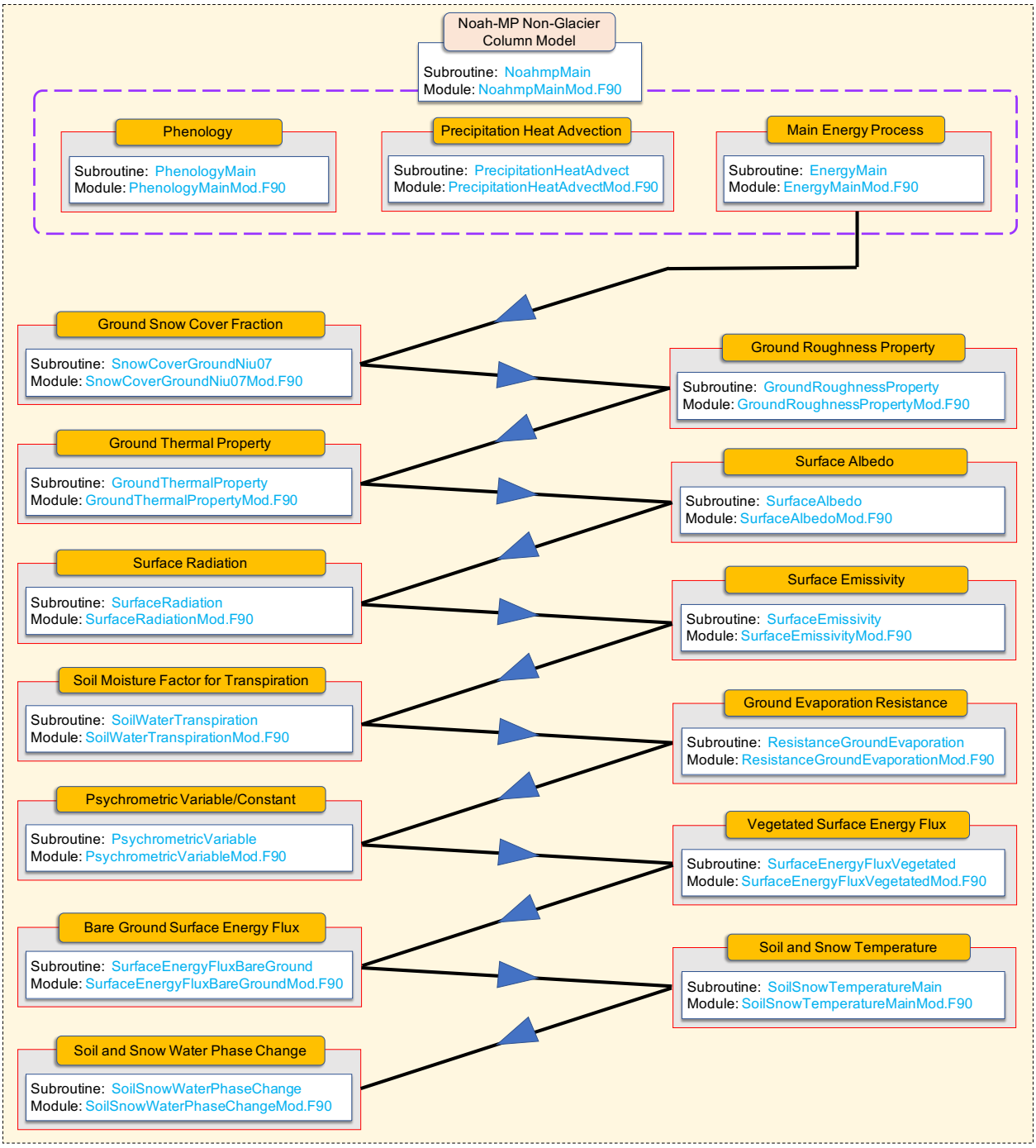

Figure 5. The modularized Noah-MP energy processes calling tree in version 5.0. Note that the glacier model has similar structures except that the vegetation-related processes are removed and soil is replaced by glacier ice.

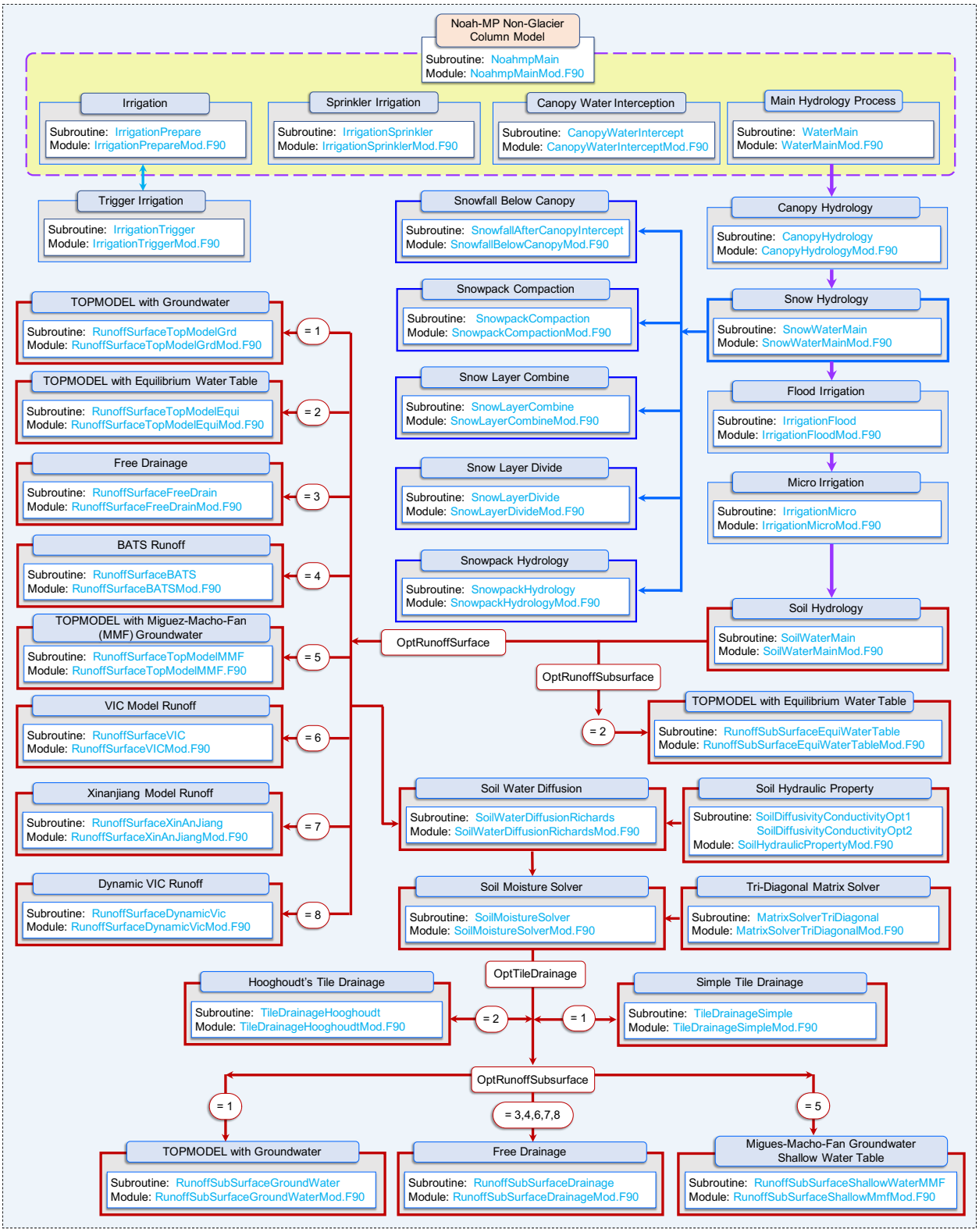

Figure 6. The modularized Noah-MP water processes calling tree in version 5.0. Note that the glacier model has similar structures except that it only includes the snowpack processes and soil is replaced by glacier ice.

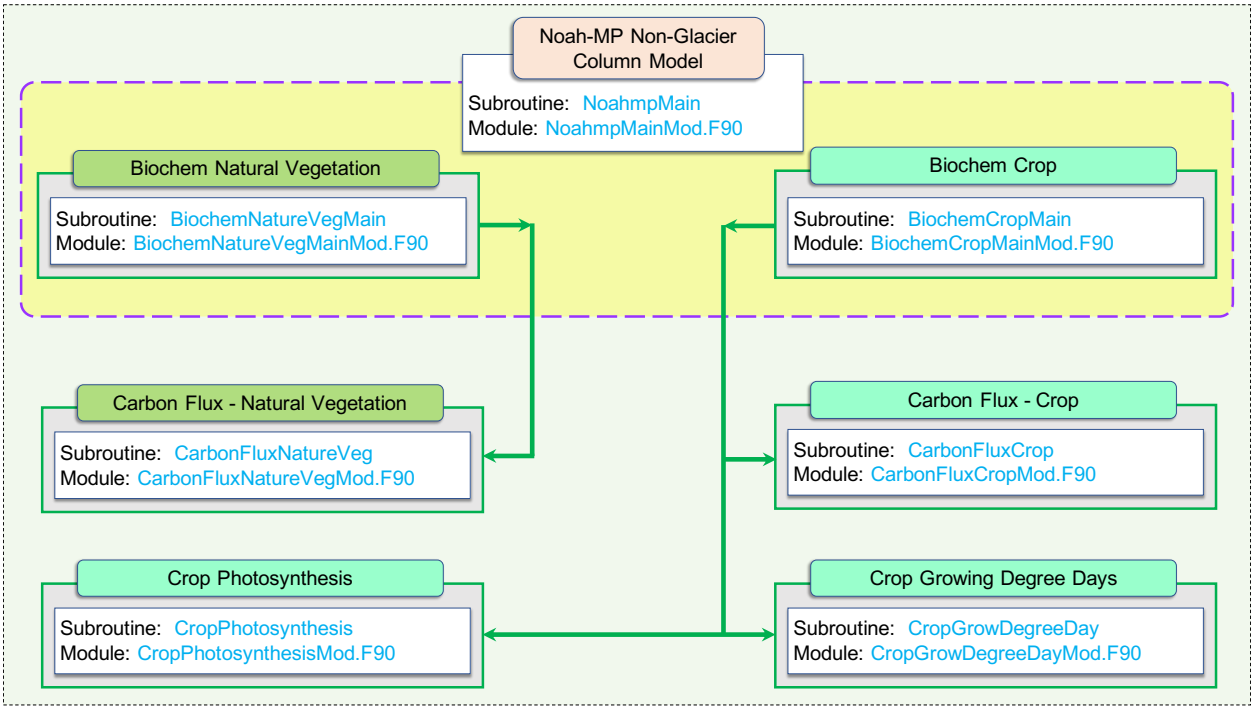

Figure 7. The modularized Noah-MP biochemical processes calling tree in version 5.0. Note that currently the Noah-MP v5.0 only includes carbon processes. Note that the CropPhotosynthesis module is not used currently to avoid inconsistency with the photosynthesis calculations from the canopy stomatal resistance module.

4. Enhanced data structure in Noah-MP version 5.0

In the Noah-MP v5.0, we have enhanced data structure with new hierarchical data types, which allows a more efficient and convenient control of model variables and substantially simplifies code structures and calling interface (Section 5). Figure 8 summarizes the new Noah-MP data type hierarchy and gives some examples of model variable expression based on the hierarchical data types. Specifically, we have defined an overarching "noahmp" main data type, which includes "forcing" for atmospheric forcing variable type, "config" for model configuration variable type with "domain" and "namelist" subtypes, "energy" for energy-related variable type, "water" for water-related variable type, and "biochem" for biochemistry-related variable type. The "energy", "water", and "biochem" types are further divided into "flux", "state", and "param" subtypes for flux, state, and parameter variables. This hierarchical data structure provides a better organization and management of model variables and their physical attributes. We have also optimized the variable declaration and initialization structures based on those new data types and consistent coding format and standard. In addition, we have re-defined many key local model state, flux, and parameter variables in the base code to be global variables in the refactored code, which allows a

better track and management of these variables for diagnosis, transfer between Noah-MP and host models, and coupling with data assimilation systems.

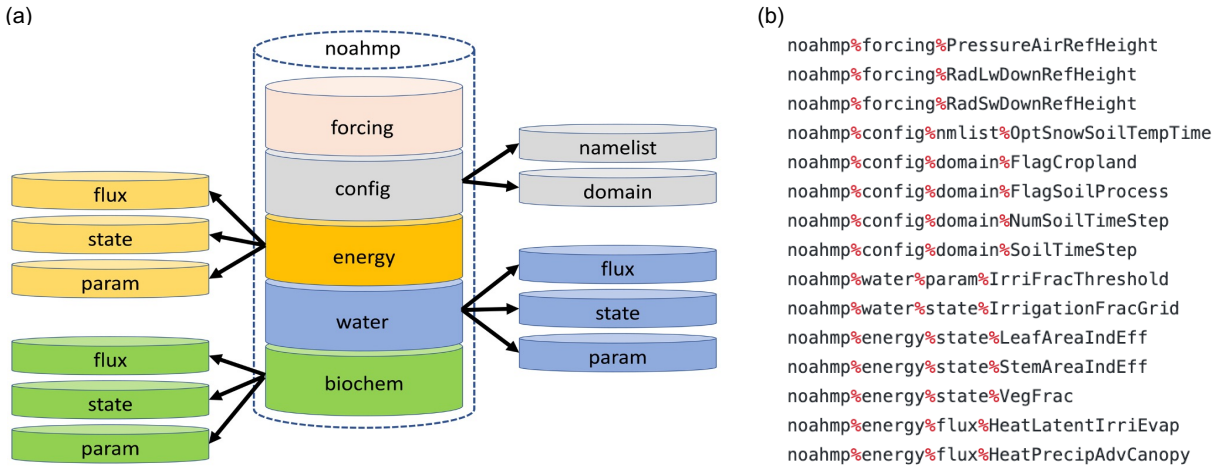

Figure 8. (a) The new hierarchical "noahmp" data types in the Noah-MP version 5.0. (b) Examples of model variable expression using the hierarchical data types.

5. Enhanced code structure in Noah-MP version 5.0

Leveraging the model modularization (Section 3) and new data types (Section 4) in the Noah-MP v5.0, we have further refined the code structure and subroutine interface. A graphical representation of the refactored Noah-MP subroutine interface is depicted in Figure 9. Specifically, the refined subroutine interface only requires passing the "noahmp" data type instead of each individual variable names, because all relevant variables are defined and included in the "noahmp" data type. This significantly simplifies the code structure with much more concise and neat subroutine calls. The refined subroutine interface also makes future model development and code changes simpler, more efficient, and less error-prone. For instance, if users want to add/remove a variable for a specific physical scheme, they only need to edit as few as 3 module files: variable type definition module, variable initialization module, the target physical scheme module, and if needed, the variable input/output module. There is no need to go through and change all the subroutine calls and interfaces that use the target variable.

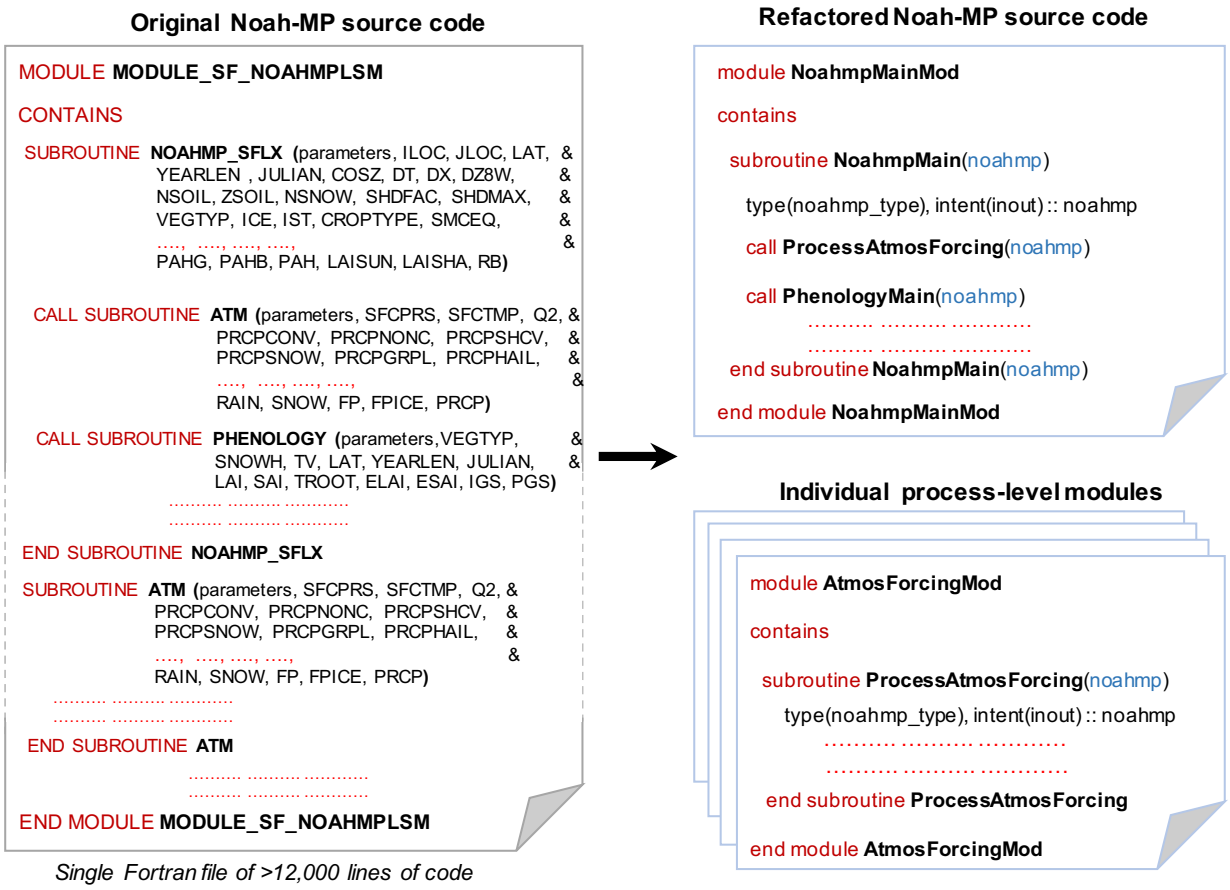

Figure 9. Demonstration of refactored subroutine interface and code structure in the Noah-MP version 5.0.

6. Enhanced variable naming in Noah-MP version 5.0

In the Noah-MP v5.0, we have also renamed all the model variables using a more descriptive and self-explanatory naming standard, which clarifies the physical meaning of variables directly by their names and hence substantially lowers the hurdles of reading and understanding the code and model physics. The original variable names in the previous Noah-MP versions are hard to understand, in which case users have to check back and forth the variable definition to know their physical meaning. For instance, the original variable name for canopy intercepted total water is "CMC", while the new name is "CanopyTotalWater". Table 2 gives more examples of the enhanced variable naming in Noah-MP v5.0. A detailed Noah-MP variable glossary listing variables' original and new names, physical meaning, data type, and unit is provided in the technical documentation (He et al., 2023) and the community Noah-MP GitHub repository.

Table 2. Examples of new variable names based on a more descriptive and self-explanatory naming standard in the Noah-MP version 5.0, compared with the original names.

Variable physical meaning/definition	New name	Original name	Variable Type	Unit
wetted or snowed fraction of canopy	CanopyWetFrac	FWET	Real	-
canopy intercepted liquid water	CanopyLiqWater	CANLIQ	Real	mm
canopy intercepted ice	CanopyIce	CANICE	Real	mm
canopy intercepted total water	CanopyTotalWater	CMC	Real	mm
canopy capacity for snow interception	CanopyIceMax	MAXSNO	Real	mm
canopy capacity for liquid water interception	CanopyLiqWaterMax	MAXLIQ	Real	mm
ice fraction in snow layers	SnowIceFrac	FICE_SNOW	Real	-
bulk density of snowfall	SnowfallDensity	BDFALL	Real	kg/m^3
snow cover fraction	SnowCoverFrac	FSNO	Real	-
snow layer ice	SnowIce	SNICE	Real	mm
snow layer liquid water	SnowLiqWater	SNLIQ	Real	mm

7. Enhanced coupling structure with host models in Noah-MP version 5.0

We have further updated the Noah-MP driver and interface coupled with potential host weather/climate/hydrology models. Figure 10 summarizes the interface and coupling structures in the Noah-MP v5.0. Specifically, the coupling interface includes: (1) defining a 2-D (for structured grid mesh) or vectorized (for unstructured grid mesh) Noah-MP input/output data type "NoahmpIO" to facilitate the input/output communication between host models and the core Noah-MP 1-D column model ("noahmp" data type); (2) the initialization of the "NoahmpIO" variables with values from host models; (3) the main Noah-MP driver that calls the core 1-D column model and transfers between the "NoahmpIO" and "noahmp" variables as part of input/output processes. Currently, the coupling of the Noah-MP v5.0 with the NCAR/HRLDAS system has been successfully completed. The coupling of Noah-MP v5.0 with the NASA/LIS system and the WRF-Hydro/NWM system is on-going. We also plan to couple the Noah-MP v5.0 with other host models in the future (Section 9), such as WRF, MPAS, and NOAA/UFS. Because of the enhanced coupling interface and structure in Noah-MP v5.0, we will only need to slightly adapt the coupling interface and driver to allow it to work with different host models. We will manage and maintain the interface and driver code for each host model in the community Noah-MP GitHub repository to ensure the compatibility between host models and updated core Noah-MP source code in the future, which will allow smooth transition and seamless synthesizing of Noah-MP updates in host models.

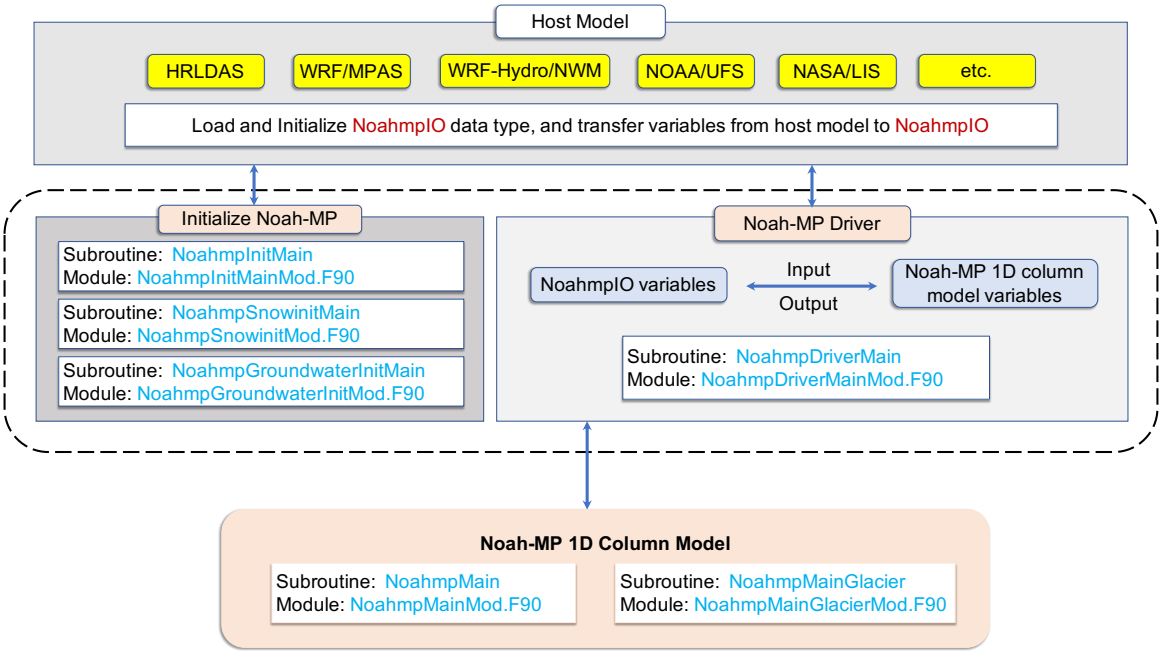

Figure 10. Workflow of the Noah-MP v5.0 driver and interface structures to couple with various host weather/climate/hydrology models.

8. Benchmarking for Noah-MP version 5.0

To benchmark the functionality, reproducibility, and computational efficiency of the modernized Noah-MP code, we have conducted a series of hierarchical test simulations during the course of Noah-MP refactoring. Specifically, after refactoring each major Noah-MP model component/physics (e.g., water, energy, carbon, etc.) listed in Figure 4, we built simple driver modules to conduct benchmark simulations using each of these model component/physics to test and ensure the bit-for-bit consistency between the refactored code and base code for all Noah-MP physics options. Here is an example for the refactored Noah-MP water component model we built for benchmarking during the course of refactoring: https://github.com/cenlinhe/NoahMP_refactor/tree/water_refactor, which was used to test the bit-for-bit consistency between the refactored and base Noah-MP water component codes.

After we completed the entire model refactoring, we have conducted another set of test simulations using the completed Noah-MP v5.0 to ensure its bit-for-bit consistency with the base model code for all different combinations of physics options as well as to benchmark its computational efficiency. These tests were conducted via 1-year point-scale SNOTEL 804-site simulations, 1-year 12-km gridded continental US simulations, and 1-year 1-km gridded simulations over central US agricultural regions (particularly to test individual and combination of physics options related to crop, irrigation, tile drainage, and groundwater). The tests all showed exactly the same results between the refactored and base simulations, with similar computational efficiency.

In addition, in order to provide the community with reference Noah-MP v5.0 model datasets for future comparison and assessment, we have conducted 3 sets of benchmark simulations, including 21-year (2000-2020) 12-km continental US simulations driven by the NLDAS-2 atmospheric forcings (Xia et al., 2012), 10-year (2009-2018) point-scale SNOTEL 804-site simulations over the western US driven by observed precipitation and temperature as well as other NLDAS-2 atmospheric forcings downscaled to 90-m spatial resolution (He et al., 2021), and 1-year (2000) 4-km dynamic crop simulations over the U.S. Corn Belt region driven by the convection-permitting WRF modeling (Zhang et al., 2020). We have archived all the atmospheric forcing datasets, model setup input datasets, and model output datasets for these benchmark simulations. Figure 11 shows an example of the model output. Note that a comprehensive evaluation of the simulation results is outside the scope of this model description paper and will be done in the next step.

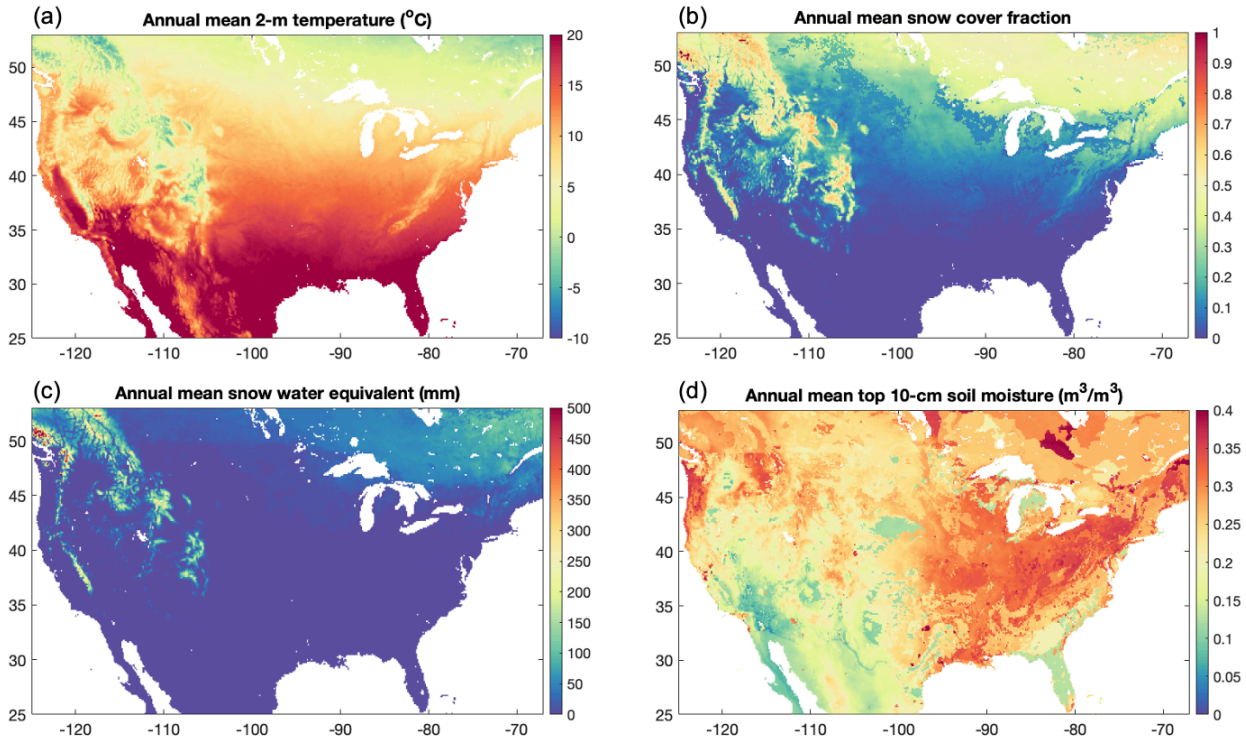

Figure 11. Demonstration of 20-year (2001-2020) annual mean (a) 2-m temperature, (b) snow cover fraction, (c) snow water equivalent, and (d) top 10-cm soil moisture from the Noah-MP version 5.0 12-km continental US benchmark simulations driven by the NLDAS-2 atmospheric forcings.

9. Model code and technical documentation for Noah-MP version 5.0

We archive, manage, and maintain the Noah-MP v5.0 (together with previous code versions) at the NCAR community Noah-MP GitHub repository (https://github.com/NCAR/noahmp) for

public access. We have also created a comprehensive technical documentation (He et al., 2023) for the Noah-MP v5.0, available at http://dx.doi.org/10.5065/ew8g-yr95, which provides detailed descriptions of model physics and formulations.

10. Conclusions and future plans

In this study, we modernized the widely-used state-of-the-art Noah-MP LSM by adopting modern Fortran 2003 code standards and data structures, which substantially enhances the model modularity, interoperability, and applicability. The modernized Noah-MP has been released as the model version 5.0, which includes the following key features: (1) enhanced modularization by re-organizing model physics into individual process-level Fortran module files, (2) enhanced data structure with new hierarchical data types and optimized variable declaration and initialization structures, (3) enhanced code structure and calling workflow by leveraging the new data structure and modularization, (4) enhanced (descriptive and self-explanatory) model variable naming standard, and (5) enhanced driver and interface structure to couple with host weather/climate/hydrology models. The base code used for modernization is the Noah-MP version 4.5 (released in December 2022), and the modernization effort does not change model physics. In addition, we have created a comprehensive technical documentation (He et al., 2023) of the Noah-MP v5.0, and a set of benchmark simulation datasets.

The Noah-MP v5.0 has been recently coupled to the NCAR/HRLDAS system and the Korean Integrated Model (KIM) system. Currently, the work of coupling the Noah-MP v5.0 with the latest NASA/LIS system and the WRF-Hydro/NWM system is on-going. The future plans for Noah-MP developments and applications include but not limited to (1) coupling with other widely-used weather/climate models (e.g., WRF, MPAS, NOAA/UFS), (2) enhancing capability of land data assimilation with Noah-MP, (3) enhancing plant hydraulics and soil hydraulics/hydrology schemes, (4) improving accuracy of applications in subseasonal-to-seasonal (S2S) forecasts, food-water security, and extreme weather/climate (e.g., fire, drought, flood, and heatwave), (5) including automated model parameter calibration/optimization algorithms, (6) enhancing modeling capabilities for rapid landscape transformation (e.g., deforestation/reforestation) as well as vegetation recovery and replacement after environmental disturbance, (7) including human management modeling (e.g., groundwater pumping), (8) including interactions with air pollution (e.g., pollutants' deposition and ozone damage to vegetation), (9) enhancing representation of subgrid heterogeneity, (10) improving high-resolution input datasets (e.g., soil properties and groundwater-related inputs), and (11) creating a set of packages for code benchmarking and testing, model diagnostic, and better debugging capability. Overall, the modernized open-source community Noah-MP model allows a more efficient and convenient process for future model developments and applications.

Code and data availability

1. The Noah-MP model code (https://doi.org/10.5281/zenodo.7901855) is available at https://github.com/NCAR/noahmp
2. The coupled HRLDAS/Noah-MP model code (https://doi.org/10.5281/zenodo.7901867) is available at https://github.com/NCAR/hrldas
3. The Noah-MP technical documentation is available at http://dx.doi.org/10.5065/ew8g-yr95
4. The benchmark datasets are stored in the NCAR high-performance supercomputer (HPC) campaign storage file system (data path: /glade/campaign/ral/hap/cenlinhe/NoahMP_benchmark/, see details about the storage system at https://arc.ucar.edu/knowledge_base/70549621) and can be provided by the corresponding author upon request, due to the extremely large data size (8.8 TB).

Author contribution

CH, PV, and MB led the code refactoring effort with the help from all the other coauthors (FC, DG, RC, GN, ZY, DN, ME, TS, RR). CH and PV led the technical documentation writing effort with the help from all the other coauthors (MB, FC, DG, RC, GN, ZY, DN, ME, TS, RR). CH conducted the benchmark model simulations. CH drafted the manuscript with improvements from all the other coauthors (PV, FC, MB, DG, RC, GN, ZY, DN, ME, TS, RR).

Competing interests

The authors declare that they have no conflict of interest.

Acknowledgements

We thank Zhe Zhang (NCAR) and Ronnie Abolafia-Rosenzweig (NCAR) for helping with model code testing and for helpful discussions. We also acknowledge the strong support from the entire Noah-MP community. This study was supported by the US Geological Survey (USGS) Water Mission Area's Integrated Water Prediction Program, NOAA's Climate Program Office's Modeling, Analysis, Predictions, and Projections Program (MAPP), and the NCAR Water System Program. National Center for Atmospheric Research (NCAR) is a major facility sponsored by the National Science Foundation (NSF) under Cooperative Agreement #1852977. Any opinions, findings, conclusions, or recommendations expressed in this publication are those of the authors and do not necessarily reflect the views of the National Science Foundation.

References

Abolafia-Rosenzweig, R., He, C., Burns, S.P., Chen, F., 2021. Implementation and Evaluation of a Unified Turbulence Parameterization Throughout the Canopy and Roughness Sublayer in

553 Noah-MP Snow Simulations. J Adv Model Earth Syst 13.
554 https://doi.org/10.1029/2021MS002665
555 Abolafia-Rosenzweig, R., He, C., Chen, F., 2022a. Winter and spring climate explains a large
556 portion of interannual variability and trend in western U.S. summer fire burned area. Environ.
557 Res. Lett. 17, 054030. https://doi.org/10.1088/1748-9326/ac6886
558 Abolafia-Rosenzweig, R., He, C., McKenzie Skiles, S., Chen, F., Gochis, D., 2022b. Evaluation
559 and Optimization of Snow Albedo Scheme in Noah-MP Land Surface Model Using In Situ
560 Spectral Observations in the Colorado Rockies. J Adv Model Earth Syst 14.
561 https://doi.org/10.1029/2022MS003141
562 Abolafia-Rosenzweig, R., He, C., Chen, F. et al. 2023a. High Resolution Forecasting of Summer
563 Drought in the Western United States. Water Resources Research, in review
564 Abolafia-Rosenzweig, R., He, C., Chen, F. et al. 2023b. Evaluating Noah-MP simulated post-fire
565 runoff and snowpack in Pacific-Northwest: challenges and future improvements, Water
566 Resources Research, in review
567 Anderson, E. A. (1976), A point energy and mass balance model of a snow cover, NOAA Tech.
568 Rep. NWS 19, 150 pp., Off. of Hydrol., Natl. Weather Serv., Silver Spring, Md.
569 Arsenault, K. R., Shukla, S., Hazra, A., Getirana, A., McNally, A., Kumar, S. V., ... & Verdin, J.
570 P. (2020). Better Advance Warnings of Drought. Bulletin of the American Meteorological
571 Society, 101(10), 899-903.
572 Ball, J. T., I. E. Woodrow, and J. A. Berry (1987), A model predicting sto- matal conductance and
573 its contribution to the control of photosynthesis under different environmental conditions, in
574 Process in Photosynthesis Research, vol. 1, edited by J. Biggins, pp. 221–234, Martinus Nijhoff,
575 Dordrecht, Netherlands.
576 Barlage, M., Tewari, M., Chen, F., Miguez-Macho, G., Yang, Z. L., & Niu, G. Y. (2015). The
577 effect of groundwater interaction in North American regional climate simulations with
578 WRF/Noah-MP. Climatic Change, 129, 485-498.
579 Barlage, M., Chen, F., Rasmussen, R., Zhang, Z., & Miguez-Macho, G. (2021). The importance
580 of scale-dependent groundwater processes in land-atmosphere interactions over the central
581 United States. Geophysical Research Letters, 48(5), e2020GL092171.
582 Blyth, E. M., Arora, V. K., Clark, D. B., Dadson, S. J., De Kauwe, M. G., Lawrence, D. M., ... &
583 Yuan, H. (2021). Advances in land surface modelling. Current Climate Change Reports, 7(2),
584 45-71.
585 Bonan, G. B. (1996), A land surface model (LSM version 1.0) for ecolog- ical, hydrological, and
586 atmospheric studies: Technical description and user's guide, NCAR Tech. Note NCAR/TN-
587 417+STR, 150 pp., Natl. Cent. for Atmos. Res., Boulder, Colo.
588 Bonan, G. B., & Doney, S. C. (2018). Climate, ecosystems, and planetary futures: The challenge
589 to predict life in Earth system models. Science, 359(6375), eaam8328.
590 https://doi.org/10.1126/science.aam8328

Brunsell, N. A., de Oliveira, G., Barlage, M., Shimabukuro, Y., Moraes, E., & Aragao, L. (2021). Examination of seasonal water and carbon dynamics in eastern Amazonia: a comparison of Noah-MP and MODIS. Theoretical and Applied Climatology, 143, 571-586.

Brutsaert, W. A. (1982), Evaporation Into the Atmosphere, 299 pp., D. Reidel, Dordrecht, Netherlands.

Cai, X., Yang, Z. L., David, C. H., Niu, G. Y., & Rodell, M. (2014). Hydrological evaluation of the Noah-MP land surface model for the Mississippi River Basin. Journal of Geophysical Research: Atmospheres, 119(1), 23-38.

Cai, X., Yang, Z. L., Fisher, J. B., Zhang, X., Barlage, M., & Chen, F. (2016). Integration of nitrogen dynamics into the Noah-MP land surface model v1. 1 for climate and environmental predictions. Geoscientific Model Development, 9(1), 1-15.

Chang, M., Cao, J., Zhang, Q., Chen, W., Wu, G., Wu, L., ... & Wang, X. (2022). Improvement of stomatal resistance and photosynthesis mechanism of Noah-MP-WDDM (v1. 42) in simulation of NO 2 dry deposition velocity in forests. Geoscientific Model Development, 15(2), 787-801.

Chen, F., & Dudhia, J. (2001). Coupling an advanced land surface–hydrology model with the Penn State–NCAR MM5 Modeling System. Part I: Model implementation and sensitivity. Monthly Weather Review, 129, 17. https://doi. org/10.1175/1520-0493(2001)129<0569:caalsh>2.0.co;2

Chen, F., Janjić, Z., & Mitchell, K. (1997). Impact of atmospheric surface-layer parameterizations in the new land-surface scheme of the NCEP Mesoscale Eta Model. Boundary-Layer Meteorology, 85, 391–421. https://doi.org/10.1023/A:1000531001463

Chen, F., Mitchell, K., Schaake, J., Xue, Y., Pan, H.-L., Koren, V., et al. (1996). Modeling of land surface evaporation by four schemes and comparison with FIFE observations. Journal of Geophysical Research: Atmospheres, 101, 7251–7268. https://doi.org/10.1029/95JD02165

Chen, F., & Zhang, Y. (2009). On the coupling strength between the land surface and the atmosphere: From viewpoint of surface exchange coefficients. Geophysical Research Letters, 36(10).

Chen, L., Li, Y., Chen, F., Barr, A., Barlage, M., & Wan, B. (2016). The incorporation of an organic soil layer in the Noah-MP land surface model and its evaluation over a boreal aspen forest. Atmospheric Chemistry and Physics, 16(13), 8375-8387.

Dickinson, R. E. (1983), Land surface processes and climate-surface albe- dos and energy balance, in Theory of Climate, Adv. Geophys., vol. 25, edited by B. Saltzman, pp. 305–353, Academic, San Diego, Calif.

Dickinson, R. E., A. Henderson-Sellers, and P. J. Kennedy (1993), Bio- sphere-Atmosphere Transfer Scheme (BATS) version 1e as coupled to the NCAR Community Climate Model, NCAR Tech. Note NCAR/TN- 387+STR, 80 pp., Natl. Cent. for Atmos. Res., Boulder, Colo.

Dickinson, R. E., M. Shaikh, R. Bryant, and L. Graumlich (1998), Interac- tive canopies for a climate model, J. Clim., 11, 2823–2836, doi:10.1175/ 1520-0442(1998)011<2823:ICFACM>2.0.CO;2.

Ek, M. B., Mitchell, K. E., Lin, Y., Rogers, E., Grunmann, P., Koren, V., et al. (2003). Implementation of Noah land surface model advances in the National Centers for

631 Environmental Prediction operational mesoscale Eta model. Journal of Geophysical Research:
632 Atmospheres, 108, 2002JD003296. https://doi.org/10.1029/2002JD003296
633 Fan, Y., Miguez-Macho, G., Weaver, C. P., Walko, R., & Robock, A. (2007). Incorporating water
634 table dynamics in climate modeling: 1. Water table observations and equilibrium water table
635 simulations. Journal of Geophysical Research: Atmospheres, 112(D10).
636 Gao, Y., Xiao, L., Chen, D., Chen, F., Xu, J., & Xu, Y. (2017). Quantification of the relative role
637 of land-surface processes and large-scale forcing in dynamic downscaling over the Tibetan
638 Plateau. Climate Dynamics, 48, 1705-1721.
639 Hazra, A., McNally, A., Slinski, K., Arsenault, K. R., Shukla, S., Getirana, A., ... & Koster, R. D.
640 (2023). NASA's NMME-based S2S hydrologic forecast system for food insecurity early
641 warning in southern Africa. Journal of Hydrology, 617, 129005.
642 He, C., F. Chen, M. Barlage, C. Liu, A. Newman, W. Tang, K. Ikeda, and R. Rasmussen (2019):
643 Can convection-permitting modeling provide decent precipitation for offline high-resolution
644 snowpack simulations over mountains, J. Geophys. Res.-Atmos,
645 124, https://doi.org/10.1029/2019JD030823
646 He, C., F. Chen, R. Abolafia-Rosenzweig, K. Ikeda, C. Liu, and R. Rasmussen (2021): What
647 causes the unobserved early-spring snowpack ablation in convection-permitting WRF modeling
648 over Utah mountains?, J. Geophys. Res.-Atmos, 126(22),
649 e2021JD035284, https://doi.org/10.1029/2021JD035284
650 He, C., P. Valayamkunnath, M. Barlage, F. Chen, D. Gochis, R. Cabell, T. Schneider, R.
651 Rasmussen, G.-Y. Niu, Z.-L. Yang, D. Niyogi, and M. Ek (2023): The Community Noah-MP
652 Land Surface Modeling System Technical Description Version 5.0. (*No. NCAR/TN-575+STR*),
653 http://dx.doi.org/10.5065/ew8g-yr95
654 Ingwersen, J., Högy, P., Wizemann, H. D., Warrach-Sagi, K., & Streck, T. (2018). Coupling the
655 land surface model Noah-MP with the generic crop growth model Gecros: Model description,
656 calibration and validation. Agricultural and forest meteorology, 262, 322-339.
657 Jarvis, P. G. (1976), The interpretation of the variations in leaf water poten- tial and stomatal
658 conductance found in canopies in the field, Philos. Trans. R. Soc. B, 273, 593–610,
659 doi:10.1098/rstb.1976.0035.
660 Jayawardena, A. W. and Zhou, M. C.: A modified spatial soil moisture storage capacity
661 distribution curve for the Xinanjiang model, Journal of Hydrology, 227, 93–113,
662 https://doi.org/10.1016/S0022-1694(99)00173-0, 2000.
663 Jiang, Y., Chen, F., Gao, Y., He, C., Barlage, M., & Huang, W. (2020). Assessment of uncertainty
664 sources in snow cover simulation in the Tibetan Plateau. Journal of Geophysical Research:
665 Atmospheres, 125(18), e2020JD032674.
666 Jiang, Y., Gao, Y., He, C., Liu, B., Pan, Y., & Li, X. (2021). Spatiotemporal distribution and
667 variation of wind erosion over the Tibetan Plateau based on a coupled land-surface wind-
668 erosion model. Aeolian Research, 50, 100699.
669 Jordan, R. (1991), A one-dimensional temperature model for a snow cover, Spec. Rep. 91–16,
670 Cold Reg. Res. and Eng. Lab., U.S. Army Corps of Eng., Hanover, N. H.

Ju, C., Li, H., Li, M., Liu, Z., Ma, Y., Mamtimin, A., ... & Song, Y. (2022). Comparison of the Forecast Performance of WRF Using Noah and Noah-MP Land Surface Schemes in Central Asia Arid Region. Atmosphere, 13(6), 927.

Koren, V., J. C. Schaake, K. E. Mitchell, Q.-Y. Duan, F. Chen, and J. M. Baker (1999), A parameterization of snowpack and frozen ground intended for NCEP weather and climate models, J. Geophys. Res., 104, 19,569–19,585, doi:10.1029/1999JD900232.

Kumar, S. V., Mocko, D. M., Wang, S., Peters-Lidard, C. D., & Borak, J. (2019). Assimilation of remotely sensed leaf area index into the Noah-MP land surface model: Impacts on water and carbon fluxes and states over the continental United States. *Journal of Hydrometeorology*, *20*(7), 1359-1377.

Kumar, S. V., Holmes, T., Andela, N., Dharssi, I., Hain, C., Peters-Lidard, C., ... & Getirana, A. (2021). The 2019–2020 Australian drought and bushfires altered the partitioning of hydrological fluxes. Geophysical Research Letters, 48(1), e2020GL091411.

Li, X., Wu, T., Zhu, X., Jiang, Y., Hu, G., Hao, J., ... & Ying, X. (2020). Improving the Noah-MP model for simulating hydrothermal regime of the active layer in the permafrost regions of the Qinghai-Tibet Plateau. Journal of Geophysical Research: Atmospheres, 125(16), e2020JD032588.

Li, J., Chen, F., Lu, X., Gong, W., Zhang, G., & Gan, Y. (2020). Quantifying contributions of uncertainties in physical parameterization schemes and model parameters to overall errors in Noah-MP dynamic vegetation modeling. Journal of Advances in Modeling Earth Systems, 12. https://doi.org/10.1029/2019MS001914

Li, L., Yang, Z. L., Matheny, A. M., Zheng, H., Swenson, S. C., Lawrence, D. M., ... & Leung, L. R. (2021). Representation of plant hydraulics in the Noah-MP land surface model: Model development and multiscale evaluation. Journal of Advances in Modeling Earth Systems, 13(4), e2020MS002214.

Li, M., Wu, P., Ma, Z., Lv, M., Yang, Q., & Duan, Y. (2022). The decline in the groundwater table depth over the past four decades in China simulated by the Noah-MP land model. Journal of Hydrology, 607, 127551.

Liang, J., Yang, Z., & Lin, P. (2019). Systematic hydrological evaluation of the Noah-MP land surface model over China. Advances in Atmospheric Sciences, 36, 1171-1187.

Liang, X., Lettenmaier, D. P., Wood, E. F., & Burges, S. J. (1994). A simple hydrologically based model of land surface water and energy fluxes for general circulation models. Journal of Geophysical Research: Atmospheres, 99(D7), 14415-14428.

Liang, X., & Xie, Z. (2003). Important factors in land–atmosphere interactions: surface runoff generations and interactions between surface and groundwater. Global and Planetary Change, 38(1-2), 101-114.

Liu, C., Ikeda, K., Rasmussen, R., Barlage, M., Newman, A. J., Prein, A. F., ... & Yates, D. (2017). Continental-scale convection-permitting modeling of the current and future climate of North America. *Climate Dynamics*, *49*, 71-95.

Liu, X., Chen, F., Barlage, M., Zhou, G., & Niyogi, D. (2016). Noah-MP-Crop: Introducing dynamic crop growth in the Noah-MP land surface model. Journal of Geophysical Research: Atmospheres, 121(23), 13-953.

McDaniel, R., Liu, Y., Valayamkunnath, P., Barlage, M., Gochis, D., Cosgrove, B. A., & Flowers, T. (2020, December). Moisture condition impact and seasonality of National Water Model performance under different runoff-infiltration partitioning schemes. In AGU Fall Meeting Abstracts (Vol. 2020, pp. H111-0028).

Miguez-Macho, G., Fan, Y., Weaver, C. P., Walko, R., & Robock, A. (2007). Incorporating water table dynamics in climate modeling: 2. Formulation, validation, and soil moisture simulation. Journal of Geophysical Research: Atmospheres, 112(D13).

Nie, W., Kumar, S. V., Arsenault, K. R., Peters-Lidard, C. D., Mladenova, I. E., Bergaoui, K., ... & Navari, M. (2022). Towards effective drought monitoring in the Middle East and North Africa (MENA) region: implications from assimilating leaf area index and soil moisture into the Noah-MP land surface model for Morocco. Hydrology and Earth System Sciences, 26(9), 2365-2386.

Niu, G.-Y., and Z.-L. Yang (2004), The effects of canopy processes on snow surface energy and mass balances, J. Geophys. Res., 109, D23111, doi:10.1029/2004JD004884.

Niu, G.-Y., Z.-L. Yang, R. E. Dickinson, and L. E. Gulden (2005), A sim- ple TOPMODEL-based runoff parameterization (SIMTOP) for use in global climate models, J. Geophys. Res., 110, D21106, doi:10.1029/ 2005JD006111.

Niu, G.-Y., and Z.-L. Yang (2006), Effects of frozen soil on snowmelt run- off and soil water storage at a continental scale, J. Hydrometeorol., 7, 937–952, doi:10.1175/JHM538.1.

Niu, G.-Y., Z.-L. Yang, R. E. Dickinson, L. E. Gulden, and H. Su (2007), Development of a simple groundwater model for use in climate models and evaluation with Gravity Recovery and Climate Experiment data, J. Geophys. Res., 112, D07103, doi:10.1029/2006JD007522.

Niu, G.-Y., Yang, Z.-L., Mitchell, K. E., Chen, F., Ek, M. B., Barlage, M., et al. (2011). The community Noah land surface model with mul- tiparameterization options (Noah-MP): 1. Model description and evaluation with local-scale measurements. Journal of Geophysical Research, 116, D12109. https://doi.org/10.1029/2010JD015139

Niu, G. Y., Fang, Y. H., Chang, L. L., Jin, J., Yuan, H., & Zeng, X. (2020). Enhancing the Noah-MP ecosystem response to droughts with an explicit representation of plant water storage supplied by dynamic root water uptake. Journal of Advances in Modeling Earth Systems, 12(11), e2020MS002062.

Oleson, K. W., et al. (2004), Technical description of the Community Land Model (CLM), NCAR Tech. Note NCAR/TN-461+STR, 174 pp., Natl. Cent. for Atmos. Res., Boulder, Colo. (Available at www.cgd.ucar.edu/ tss/clm/distribution/clm3.0/index.html.)

Patel, P., Jamshidi, S., Nadimpalli, R., Aliaga, D. G., Mills, G., Chen, F., ... & Niyogi, D. (2022). Modeling Large-Scale Heatwave by Incorporating Enhanced Urban Representation. Journal of Geophysical Research: Atmospheres, 127(2), e2021JD035316.

Sakaguchi, K., & Zeng, X. (2009). Effects of soil wetness, plant litter, and under-canopy atmospheric stability on ground evaporation in the Community Land Model (CLM3. 5). Journal of Geophysical Research: Atmospheres, 114(D1).

Salamanca, F., Zhang, Y., Barlage, M., Chen, F., Mahalov, A., & Miao, S. (2018). Evaluation of the WRF-urban modeling system coupled to Noah and Noah-MP land surface models over a semiarid urban environment. Journal of Geophysical Research: Atmospheres, 123(5), 2387-2408.

Saxton, K. E., & Rawls, W. J. (2006). Soil water characteristic estimates by texture and organic matter for hydrologic solutions. Soil science society of America Journal, 70(5), 1569-1578.

Sellers, P. J. (1985), Canopy reflectance, photosynthesis and transpiration, Int. J. Remote Sens., 6, 1335–1372, doi:10.1080/01431168508948283.

Sellers, P. J., M. D. Heiser, and F. G. Hall (1992), Relations between surface conductance and spectral vegetation indices at intermediate (100 m2 to 15 km2) length scales, J. Geophys. Res., 97, 19,033–19,059, doi:10.1029/92JD01096.

Schaake, J. C., V. I. Koren, Q.-Y. Duan, K. E. Mitchell, and F. Chen (1996), Simple water balance model for estimating runoff at different spatial and temporal scales, J. Geophys. Res., 101, 7461–7475, doi:10.1029/95JD02892.

Shu, Z., Zhang, B., Tian, L., & Zhao, X. (2022). Improving Dynamic Vegetation Modeling in Noah‐MP by Parameter Optimization and Data Assimilation Over China's Loess Plateau. *Journal of Geophysical Research: Atmospheres*, *127*(19), e2022JD036703.

Suzuki, K., & Zupanski, M. (2018). Uncertainty in solid precipitation and snow depth prediction for Siberia using the Noah and Noah-MP land surface models. Frontiers of Earth Science, 12, 672-682.

Valayamkunnath, P., Chen, F., Barlage, M. J., Gochis, D. J., Franz, K. J., & Cosgrove, B. A. (2021, January). Impact of Agriculture Management Practices on the National Water Model Simulated Streamflow. In 101st American Meteorological Society Annual Meeting. AMS.

Valayamkunnath, P., Gochis, D. J., Chen, F., Barlage, M., & Franz, K. J. (2022). Modeling the hydrologic influence of subsurface tile drainage using the National Water Model. Water Resources Research, 58(4), e2021WR031242.

Verseghy, D. L. (1991), CLASS-A Canadian land surface scheme for GCMS: I. Soil model, Int. J. Climatol., 11, 111–133, doi:10.1002/joc.3370110202.

Wang, P., Niu, G. Y., Fang, Y. H., Wu, R. J., Yu, J. J., Yuan, G. F., ... & Scott, R. L. (2018). Implementing dynamic root optimization in Noah-MP for simulating phreatophytic root water uptake. Water Resources Research, 54(3), 1560-1575.

Wang, W., Yang, K., Zhao, L., Zheng, Z., Lu, H., Mamtimin, A., ... & Moore, J. C. (2020). Characterizing surface albedo of shallow fresh snow and its importance for snow ablation on the interior of the Tibetan Plateau. Journal of Hydrometeorology, 21(4), 815-827.

Wang, W., He, C., Moore, J., Wang, G., & Niu, G. Y. (2022). Physics-Based Narrowband Optical Parameters for Snow Albedo Simulation in Climate Models. Journal of Advances in Modeling Earth Systems, 14(1), e2020MS002431.

Wang, Y. H., Broxton, P., Fang, Y., Behrangi, A., Barlage, M., Zeng, X., & Niu, G. Y. (2019). A wet-bulb temperature-based rain-snow partitioning scheme improves snowpack prediction over the drier western United States. Geophysical Research Letters, 46(23), 13825-13835.

Warrach-Sagi, K., J. Ingwersen, T. Schwitalla, C. Troost, J. Aurbacher, L. Jach, T. Berger, T. Streck, and V. Wulfmeyer, 2022: Noah-MP with the generic crop growth model Gecros in the WRF model: Effects of dynamic crop growth on land-atmosphere interaction. J Geophys Res-Atmos, 127(14), e2022JD036518.DOI:10.1029/2022JD036518

Wrzesien, M. L., Pavelsky, T. M., Kapnick, S. B., Durand, M. T., & Painter, T. H. (2015). Evaluation of snow cover fraction for regional climate simulations in the S ierra N evada. International Journal of Climatology, 35(9), 2472-2484.

Wu, W. Y., Yang, Z. L., & Barlage, M. (2021). The Impact of Noah-MP Physical Parameterizations on Modeling Water Availability during Droughts in the Texas–Gulf Region. Journal of Hydrometeorology, 22(5), 1221-1233.

Xia, Y., K. Mitchell, M. Ek, J. Sheffield, B. Cosgrove, E. Wood, L. Luo, C. Alonge, H. Wei, J. Meng, B. Livneh, D. Lettenmaier, V. Koren, Q. Duan, K. Mo, Y. Fan, and D. Mocko (2012). Continental-scale water and energy flux analysis and validation for the North American Land Data Assimilation System project phase 2 (NLDAS-2): 1. Intercomparison and application of model products. J. Geophys. Res., 117, D03109, doi:10.1029/2011JD016048

Xu, T., Chen, F., He, X., Barlage, M., Zhang, Z., Liu, S., & He, X. (2021). Improve the performance of the noah-MP-crop model by jointly assimilating soil moisture and vegetation phenology data. Journal of Advances in Modeling Earth Systems, 13(7), e2020MS002394.

Xu, X., Chen, F., Shen, S., Miao, S., Barlage, M., Guo, W., & Mahalov, A. (2018). Using WRF-urban to assess summertime air conditioning electric loads and their impacts on urban weather in Beijing. Journal of Geophysical Research: Atmospheres, 123(5), 2475-2490.

Xue, Y., P. J. Sellers, J. L. Kinter, and J. Shukla (1991), A simplified bio- sphere model for global climate studies, J. Clim., 4, 345–364, doi:10.1175/1520-0442(1991)004<0345:ASBMFG>2.0.CO;2.

Yang, Z.-L., and R. E. Dickinson (1996), Description of the Biosphere- Atmosphere Transfer Scheme (BATS) for the soil moisture workshop and evaluation of its performance, Global Planet. Change, 13, 117–134, doi:10.1016/0921-8181(95)00041-0.

Yang, Z. L., Niu, G. Y., Mitchell, K. E., Chen, F., Ek, M. B., Barlage, M., ... & Xia, Y. (2011). The community Noah land surface model with multiparameterization options (Noah-MP): 2. Evaluation over global river basins. Journal of Geophysical Research: Atmospheres, 116(D12).

Yen, Y. C. (1965). Effective thermal conductivity and water vapor diffusivity of naturally compacted snow. Journal of Geophysical Research, 70(8), 1821-1825.

Yen, Y. C. (1981). Review of thermal properties of snow, ice, and sea ice (Vol. 81, No. 10). US Army, Corps of Engineers, Cold Regions Research and Engineering Laboratory.

Zhang, G., Chen, F., & Gan, Y. (2016). Assessing uncertainties in the Noah-MP ensemble simulations of a cropland site during the Tibet Joint International Cooperation program field

campaign. Journal of Geophysical Research: Atmospheres, 121, 9576–9596. https://doi.org/10.1002/2016JD024928

Zhang, X. Y., Jin, J., Zeng, X., Hawkins, C. P., Neto, A. A., & Niu, G. Y. (2022a). The compensatory CO2 fertilization and stomatal closure effects on runoff projection from 2016–2099 in the western United States. Water Resources Research, 58(1), e2021WR030046.

Zhang, X., Xie, Z., Ma, Z., Barron-Gafford, G. A., Scott, R. L., & Niu, G. Y. (202b). A Microbial-Explicit Soil Organic Carbon Decomposition Model (MESDM): Development and Testing at a Semiarid Grassland Site. Journal of Advances in Modeling Earth Systems, 14(1), e2021MS002485.

Zhang, Z., Barlage, M., Chen, F., Li, Y., Helgason, W., Xu, X., ... & Li, Z. (2020). Joint modeling of crop and irrigation in the central United States using the Noah-MP land surface model. Journal of Advances in Modeling Earth Systems, 12(7), e2020MS002159.

Zhang, Z., Chen, F., Barlage, M., Bortolotti, L. E., Famiglietti, J., Li, Z., ... & Li, Y. (2022). Cooling Effects Revealed by Modeling of Wetlands and Land-Atmosphere Interactions. Water Resources Research, 58(3), e2021WR030573.

Zhang, Z., Li, Y., Chen, F., Harder, P., Helgason, W., Famiglietti, J., Valayamkunnath, P., He, C., and Li, Z.: Developing Spring Wheat in the Noah-MP LSM (v4.4) for Growing Season Dynamics and Responses to Temperature Stress, Geosci. Model Dev. Discuss. [preprint], https://doi.org/10.5194/gmd-2022-311, in review, 2023.

Zhuo, L., Dai, Q., Han, D., Chen, N., & Zhao, B. (2019). Assessment of simulated soil moisture from WRF Noah, Noah-MP, and CLM land surface schemes for landslide hazard application. Hydrology and Earth System Sciences, 23(10), 4199-4218.

Zonato, A., Martilli, A., Gutierrez, E., Chen, F., He, C., Barlage, M., ... & Giovannini, L. (2021). Exploring the effects of rooftop mitigation strategies on urban temperatures and energy consumption. Journal of Geophysical Research: Atmospheres, 126(21), e2021JD035002.